arXiv:nucl-th/9904073v1 28 Apr 1999

Tri-axial Octupole Deformations and Shell Structure

W.D. Heiss[1], R.G. Nazmitdinov[1,2] and R.A. Lynch[1]

[1] Centre for Nonlinear Studies and Department of Physics

University of the Witwatersrand, PO Wits 2050, Johannesburg, South Africa

[2] Bogoliubov Laboratory of Theoretical Physics

Joint Institute for Nuclear Research, 141980 Dubna, Russia

Manifestations of pronounced shell effects are discovered when adding nonaxial octupole deformations to a harmonic oscillator model. The degeneracies of the quantum spectra are in a good agreement with the corresponding main periodic orbits and winding number ratios which are found by classical analysis.

PACS numbers: 21.60.-n, 05.45.+b, 21.10.-k, 36.40.-c

The remarkable regularity of rotational spectra of superdeformed nuclei has prompted many investigations into the contribution of higher multipoles on the formation of shell structure [1]. Related questions have arisen for other mesoscopic systems. In particular, it appears that octupole deformation has the same importance for two-dimensional systems like quantum dots and surface clusters [2] as for three-dimensional systems like nuclei [3] and metallic clusters [4]. Semi-classical analysis based on periodic orbit theory [5–7] provides substantial insight into the role of the octupole deformation for axially symmetric systems [8–10]. Axially symmetric octupole deformation which leads to soft chaos in the classical case produces short periodic orbits at particular parameter strengths, and, correspondingly, pronounced shell effects arise in the quantum spectrum [8,9].

Conservation of angular momentum may increase the regular region for a non-integrable problem with axial symmetry (see for example [11]). The situation becomes more complicated for nonaxial systems with three degrees of freedom, since angular momentum is no longer a constant of motion and the classical dynamics may lead to a stronger degree of chaos [12]. Inclusion of exotic, i.e. nonaxial, octupole deformations renders the finding of

pronounced shell effects rather difficult. Results based on the term $Y_{3\pm1}$, which was suggested by Mottelson [13] and studied in [14], have been questioned in [15]. Other attempts which incorporate nonaxial octupole deformation start with axially symmetric potentials; they have found indications of shell effects using $Y_{3\mu}$ deformations mainly with $\mu = 0, 2$ [15,16]. The increasing accuracy of measurements of nuclear spectra, due to the new generation of detectors, gives substantial indications of strong octupole correlations [3,17]. This calls for a thorough analysis of nonaxial octupole deformations. A similar question about shell effects in electronic structures and their connection to octupole deformations arises from the *ab initio* calculations of the melting transitions in small alkali clusters [18]. In this Letter we demonstrate the existence of strong shell effects which arise in the tri-axial harmonic oscillator combined with nonaxial octupole deformations. The model may serve as a simple and transparent study of the effective mean field for mesoscopic systems like nuclei and metallic clusters. In addition, features characteristic of realistic potentials, i.e. a coexistence of regular and chaotic dynamics and the consequences for quantum mechanics, are addressed.

Similar to the procedure pursued in [8] we are guided by the study of the classical motion in obtaining the quantum mechanical results. The single–particle Hamiltonian considered reads

$$H = \frac{(\vec{p})^2}{2m} + \frac{m\omega^2}{2}\left[(\frac{x}{a})^2 + (\frac{y}{b})^2 + (\frac{z}{c})^2 + r^2 \sum_{\mu} \lambda_{3\mu} Y_{3\mu}\right] \tag{1}$$

where the $Y_{\lambda\mu}$ are the usual spherical harmonics. To maintain time reversal invariance, only the combinations $Y_{3\mu} \pm Y_{3-\mu}$ are considered, with a factor i where appropriate. We take into account only one of the deformation $\mu = 0, 1, 2, 3$ at a time. For convenience, we express all quantities below in units of $\omega \equiv \omega_x$, i.e. $a = 1$. If any of the parameters $\lambda_{3\mu}$ are nonzero, we are faced with a non-integrable system. In fact, the problem gives rise to chaotic motion even at relatively small values of the octupole parameters. The parameters have to be limited by their respective critical values $\lambda_{3\mu}^{crit}$ at which the potential no longer binds. The critical values depend on the parameters a, b, c which can be expressed through standard quadrupole

deformations $\epsilon_{2\mu}$ and, if more than one $\lambda_{3\mu}$ is considered, critical surfaces are obtained. It is obvious that a search for shell structure for the corresponding quantum mechanical problem becomes meaningless above the critical values as then the quantum mechanical spectrum obtained by matrix diagonalisation does not relate to the corresponding classical Hamiltonian.

The quadrupole shapes as determined by the parameters a, b, c are illustrated by the hexagonal figure given in Fig.1. The three axes denoting axially symmetric prolate (oblate) shapes differ by an appropriate permutation of the coordinates $x-y-z$. For physical consideration it is therefore sufficient to consider just one sector if only quadrupole deformation is being studied [6]. However, the addition of an octupole term defines an orientation, since it refers to a specific z-axis. Therefore, when adding, say, the term $r^2\lambda_{30}Y_{30}$, the physical situation is different for two oblate cases, for example, *obl*$/x$ and *obl*$/z$ in Fig.1. Note that the latter case would preserve axial symmetry, thus making it effectively a two degrees of freedom system. But the former case is now a genuine three degrees of freedom system, since the symmetry axis of the quadrupole shape (the x-axis) is different from the symmetry axis of $r^2\lambda_{30}Y_{30}$ (the z-axis).

In the same vein, the addition of a term $r^2\lambda_{3\mu}Y_{3\pm\mu}$ to any of the axially symmetric quadrupole shapes, gives rise to a three degrees of freedom system for $\mu \neq 0$.

The effect of r^2Y_{30} upon the axes pro/z and *obl*$/z$ has been dealt with in [8]. We here begin with the combination $r^2(Y_{33}-Y_{3-3})$. It appears from numerical analysis of the classical equations of motion (see below) that the most regular motion occurs in the vicinity of the pro/x axis. The procedure to approximate the non-integrable classical system is the 'removal of resonances' method [19]. To lowest order it consists of averaging the Hamilton function over the fastest angle of the unperturbed motion (all $\lambda_{3\mu}=0$) after rewriting the momenta and coordinates in terms of action–angle variables, *viz.*

$$q_i = \sqrt{\tfrac{2J_i}{m\omega_i}}\sin\theta_i, \quad p_i = \sqrt{2J_i m\omega_i}\cos\theta_i,$$

$$\theta_i = \omega_i t, \quad i = x, y, z.$$

On the axis pro/x one would therefore average over θ_z or θ_y and above it over θ_z, since there $\omega_z > \omega_y > \omega_x$ $(a > b > c)$. Based on the observation that $r^2(Y_{33} - Y_{3-3})$ is proportional to $x(x^2 - 3y^2)/r$, we expect the z-motion to be weakly affected by this term. In the vicinity of the pro/x axis an averaging over θ_z is thus indicated. Moreover, for the reasons just given, an averaging over θ_z, which yields an effective potential in the $x - y$-coordinates, is expected to make little difference from an effective potential obtained by simply setting $z = 0$. This expectation is convincingly confirmed by numerical tests as long as $\omega_z \geq \omega_y$. In other words, for $\omega_z \geq \omega_y > \omega_x$, the motion effectively decouples into an unperturbed motion in the z-coordinate (governed by the potential $mz^2\omega^2/(2c^2)$) and the two degrees of freedom motion in the $x - y$-plane. Averaging now over the fast angle θ_y yields the unperturbed motion in the y-coordinate (governed by $my^2\omega^2/(2b^2)$) and the effective potential for x which reads

$$U_{\text{eff}}(x) = \tfrac{m\omega^2}{2}[x^2 + \lambda_{33}\tfrac{\text{sign}(x)}{\pi}(2x^2 K(-\tfrac{\xi_y^2}{x^2}) - 3\pi\xi_y^2 {}_2F_1(\tfrac{1}{2}, \tfrac{3}{2}, 2; -\tfrac{\xi_y^2}{x^2}))] \tag{2}$$

where K and ${}_2F_1$ denote the first elliptic integral and the hypergeometric function, respectively, and $\xi_y^2 = 2E_y/(m\omega_y^2)$ where $\omega_y = \omega/b$. The approximation used here assumes that E_y, the energy residing in the y-motion, is constant (and therefore also E_x); note that the effective potential $U_{\text{eff}}(x)$ depends on E_y. A numerical comparison between the true three dimensional motion and the approximate decoupled motion nicely confirms the validity of the approximation for $\lambda_{33} \lesssim \lambda_{\text{crit}}/2$. The crucial test which is relevant for the corresponding quantum mechanical case is the comparison of the winding number ratios $\omega_x^{\text{eff}}/\omega_y$ and $\omega_x^{\text{eff}}/\omega_z$. Moreover, these ratios are virtually independent of E_y for E_y less than 60% of its maximal value E_{tot}. As a result, we may evaluate analytically ω_x^{eff} by choosing $E_y = 0$ in Eq.(2) and obtain

$$\omega_x^{\text{eff}} : \omega_y : \omega_z = \frac{2\sqrt{1 - \lambda_{33}^2}}{\sqrt{1 - \lambda_{33}} + \sqrt{1 + \lambda_{33}}} : \frac{1}{b} : \frac{1}{c} \tag{3}$$

By appropriately tuning the parameters b, c and λ_{33}, we can obtain simple ratios for the winding numbers. They determine short periodic orbits which are expected to occupy a

major part of a phase space.

For a two–dimensional problem the Poincaré surface of section can be used for the estimation of the percentage of phase space occupied by periodic orbits. In the present situation, the five dimensional phase space renders an understanding of the underlying structure rather difficult. The technique utilized here is essentially a frequency analysis. It is in principle impossible to determine whether a trajectory is quasi-periodic or chaotic merely by looking at the frequency spectra [20]. A pragmatic approach is adopted here in that an initial condition is deemed to yield a chaotic orbit if the associated frequency spectra have sufficiently many discernible peaks. We call an orbit chaotic if any one of the frequency spectra has more than six peaks with intensities greater than 1% of the maximum intensity. These arbitrary choices proved satisfactory for our purpose. If the orbit is quasi-periodic, then the most significant frequency peaks are compared, and the approximate winding number and period obtained. Repeating this procedure many times using different initial conditions in phase space yields a Monte-Carlo type estimate of the portions of phase space characterized by the various different frequency ratios. If a particular simple ratio dominates, as exemplified below, then we expect specific signatures in the quantum spectrum as shell structure. Examples are illustrated in Figs.2–4. We have chosen the numbers $a : b : c = 1 : 0.5577 : 0.5577, 1 : 0.3718 : 0.5577$ to obtain the ratios $1 : 2 : 2, 1 : 3 : 2$ from Eq.(3), respectively. This ratio is sufficiently simple to make an easy comparison with the quantum results.

The adiabatic approach predicts orbits with the frequency ratios $1 : 2 : 2$ and $1 : 3 : 2$ at $\lambda_{33} = 0.5\lambda_{crit}$. The corresponding spectra are displayed in Fig.**??**. The classical frequency analysis (CFA) of the exact orbits shows a peak at $\lambda_{33} \approx 0.55\lambda_{33}^{crit}$ for the ratios $1 : 2 : 2$,$1 : 3 : 2$, and the quantum shell structure occurring at $\lambda_{33} \approx 0.5\lambda_{33}^{crit}$ has the correct degeneracy pattern for about the first hundred levels.

As a quantitative measure for shell structure we use the Strutinsky-type analysis introduced in [8]. From the quantity $\Delta E(\lambda, N) = \delta E(\lambda, N + 1) + \delta E(\lambda, N - 1) - 2\delta E(\lambda, N)$, where δE is the fluctuating part of the total energy, we obtain the precise location of the

magic numbers (see Fig.4). Similarly, the whole discussion can also be applied to the axis pro/y in Fig.1 by using the combination $r^2(Y_{33}+Y_{3-3}) \sim y(y^2-3x^2)/r$ instead. It appears that, due to the weak z-dependence of the combinations $r^2(Y_{33} \pm Y_{3-3})$, mainly the $x-y$ profile of the unperturbed harmonic oscillator is important. The stronger the deformation in the $x-y$-plane, i.e. the further away from the z-axial symmetry line (pro/z and obl/z), the better the adiabatic approximation and shell structure becomes. In contrast, along this horizontal line either $Y_{3\pm3}$ combination acts upon a circular potential in the $x-y$-plane and quickly introduces chaos.

The CFA, applied to the combination $r^2(Y_{31}-Y_{3-1}) \sim x(4z^2-x^2-y^2)$, reveals that the y motion is weakly affected for $\lambda_{31} \lesssim 0.6\lambda_{31}^{crit}$ in the vicinity of the pro/x axis. Applying the analysis described above, we found that this term leads to shell effects similar to those of $r^2(Y_{33}-Y_{3-3})$. In fact, Eq.(3) holds for this combination as well. The plus combination $r^2(Y_{31}+Y_{3-1})$ is simply the minus combination under the interchange of x and y, and thus will produce the same effects near the region pro/y. It is important to note that the addition of a term $\lambda_{30}r^2Y_{30}$ to either situation, pro/x or pro/y, leads to an onset of chaos for rather small values of λ_{30}, and accordingly the quantum spectrum does not exhibit shell structure.

The two combinations $r^2(Y_{3\mu} \pm Y_{3-\mu})$ produce the same potential shape for the spherical case [16]. However, according to the analysis above, the plus and minus combinations have different effects for different sectors of the hexagonal figure (Fig.1). The CFA shows that the adding of the octupole term $\lambda_{32}r^2(Y_{32}+Y_{3-2})$ gives rise to chaotic motion for comparatively small coupling values. In contrast, the term $\lambda_{32}r^2(Y_{32}-Y_{3-2})$ has less impact on the unperturbed motion, chaotic motion only becoming discernible for $\lambda_{32} \gtrsim 0.5\lambda_{\rm crit}$. Since $(Y_{32}-Y_{3-2})$ is symmetric with respect to an interchange of x and y, this result applies to the region above and below the axis pro/z including the axes obl/x and obl/y. The quantum mechanical results are in accordance with the classical findings: the plain quadrupole spectrum changes weakly over a considerable range of λ_{32} when adding the term $r^2(Y_{32}-Y_{3-2})$ while the order soon decays when the plus combination is switched on.

The cases considered here represent novel examples of *three–dimensional* non-integrable

systems, which can be well-approximated by integrable ones. The results of the current literature are limited primarily to axially symmetric non-integrable systems [7,12]. Special values of parameters, found with the 'removal of resonances' method, produce potentials conducive to regular classical motion in much of phase space. The various octupole combinations may have different effects on the generation of shell structure, depending on where the unperturbed potential lies in the hexagonal figure (Fig.1). The effect of r^2Y_{30} upon the axis pro/z is similar to that of $r^2(Y_{33} \pm Y_{3-3})$ and $r^2(Y_{31} \pm Y_{3-1})$ upon the axis pro/x or pro/y. In contrast, the terms $r^2(Y_{32} \pm Y_{3-2})$ do not support shell structure. In this context we mention that the special combination $r^2\tilde{\lambda}(Y_{30} + 3(Y_{32} + Y_{3-2}))$, when added to pro/z, is, after suitable permutation of the coordinates, identically equivalent to the adding of $r^2\lambda_{33}(Y_{33} - Y_{3-3})$ to pro/x. Thus, we have generalized our previous result [8] to the domain of triaxiality in that the combination of quadrupole and *nonaxial* octupole deformations has been shown to lead to shell effects equivalent to those from a plain quadrupole deformed potential, at least for the first one hundred levels. More comprehensive details of the classical frequency analysis, the adiabatic approach and the quantum mechanical analysis will be presented in a forthcoming paper. Finally, we note that negative parity states observed in rare-earth nuclei with neutron number $N \sim 92$, which become yrast at high spins, need an unexpectedly strong degree of triaxiality (see [21]) when described in terms of quadrupole and hexadecapole deformations only. We suggest that inclusion of an octupole deformation $r^2(Y_{33} - Y_{3-3})$ or a banana-type octupole deformation $r^2(Y_{31} - Y_{3-1})$ which effectively gives rise to shell effects of a tri-axial oscillator, could yield a more natural explanation of these phenomena.

R.G.N. acknowledges financial support from the Foundation for Research Development of South Africa which was provided under the auspices of the Russian/South African Agreement on Science and Technology.

---

[1] S.Åberg, H. Flocard and W. Nazarewicz, Annu. Rev. Nucl. Part. Sci. **40**, 439 (1990)

[2] S.M. Reiman *et al*, Phys.Rev. **B56**, 12147 (1997)

[3] P.A. Butler and W. Nazarewicz, Rev.Mod.Phys. **68**, 349 (1996)

[4] S.Frauendorf and V.V. Pashkevich , Ann.Physik (Berlin) **5**, 34 (1996); B. Montag *et al*, Phys.Rev. **B52**, 4775 (1995); H.Häkkinen *et al*, Phys.Rev.Lett. **78**, 1034 (1997)

[5] M.C. Gutzwiller, J.Math.Phys. **12**, 343 (1971); R. Balian and C. Bloch, Ann.Phys. (NY) **69**, 76 (1972); V.M. Strutinsky *et al*, Z.Phys. **A283**, 269 (1977)

[6] A. Bohr and B. Mottelson, *Nuclear Structure* (Benjamin, New York, 1975), Vol.2

[7] see for a recent survey M. Brack and R.K. Bhaduri, *Semiclassical Physics* (Addison and Wesley, Reading, 1997)

[8] W.D. Heiss, R.G. Nazmitdinov and S.Radu, Phys.Rev.Lett. **72**, 2351 (1994); Phys.Rev. **B51**, 1874 (1994); Phys.Rev. **C52**, 3032 (1995)

[9] K. Arita and K. Matsuyanagi, Progr.Theor.Phys. **91**, 723 (1994); Nucl.Phys. **A592**, 9 (1995)

[10] S.C. Creagh, Ann.Phys. (N.Y.) **248**, 60 (1996)

[11] W.D. Heiss and R.G. Nazmitdinov, Physica **D118**, 134 (1998)

[12] M.C. Gutzwiller, *Chaos and Classical and Quantum Mechanics* (Springer, New York, 1990)

[13] B.R. Mottelson, Proc. Conf.on High-spin nuclear structure and novel nuclear shapes. Argonne National Laboratory. ANL-PHY-88-2, p.1.

[14] R.R. Chasman, Phys.Lett. **B266**, 243 (1991)

[15] J. Skalski, Phys.Lett. **B274**, 1 (1992)

[16] I. Hamamoto *et al*, Z.Phys. **D21**,163 (1991); F.Frisk *et al*, Physica Scripta, **50**, 628 (1994)

[17] J.K. Hwang *et al*, Phys.Rev. **C56**, 1344 (1997); G.J. Lane *et al*, Phys.Rev. **C57**, R1022 (1998);

J.F. Smith *et al*, Phys.Rev. **C57**, R1037 (1998)

[18] A. Rytkönen, H. Häkkinen and M. Manninen, Phys.Rev.Lett. **80**, 3940 (1998)

[19] A.J. Lichtenberg and M.A. Lieberman, *Regular and Stochastic Motion* (Springer, New York, 1983)

[20] R.S. Dumont and P. Brumer, J.Chem.Phys. **88**, 1481 (1988)

[21] K.P. Blume *et al*, Nucl.Phys. **464**, 445 (1987); J.N. Mo *et al*, Nucl.Phys. **A472**, 295 (1987); W. Schmitz *et al*, Nucl.Phys. **A539**, 112 (1992); H.Schack-Peterson *et al*, Nucl.Phys. **A594**, 175 (1995)

Figure Captions

Fig.1 Shapes in the a, b, c plane. Spherical symmetry ($a = b = c$) is at the center while axially symmetric prolate and oblate shapes are obtained along the various axes. A genuine tri-axial quadrupole deformation ($a \neq b \neq c$) occurs between the axes.

Fig.2 Two quantum spectra: (a) for the parameters $b = c = 0.5577$; (b) for the parameters $b = 0.3718$, $c = 0.5577$. Energies are given in units of $\hbar\omega$.

Fig.3 Classical phase space occupation for the frequency ratios 1.1:3:2 and 1:3:2. The 1:3:2 peak at $\lambda_{33}/\lambda_{33}^{crit} \approx 0.55$ leads to the shell structure displayed in Fig.2b.

Fig.4 Magic numbers calculated at values of parameters as for Fig.2. The magic numbers corresponding to a pure quadrupole deformed harmonic oscillator are indicated in (a) for the ratio $1:2:2$ and in (b) for the ratio $1:3:2$.

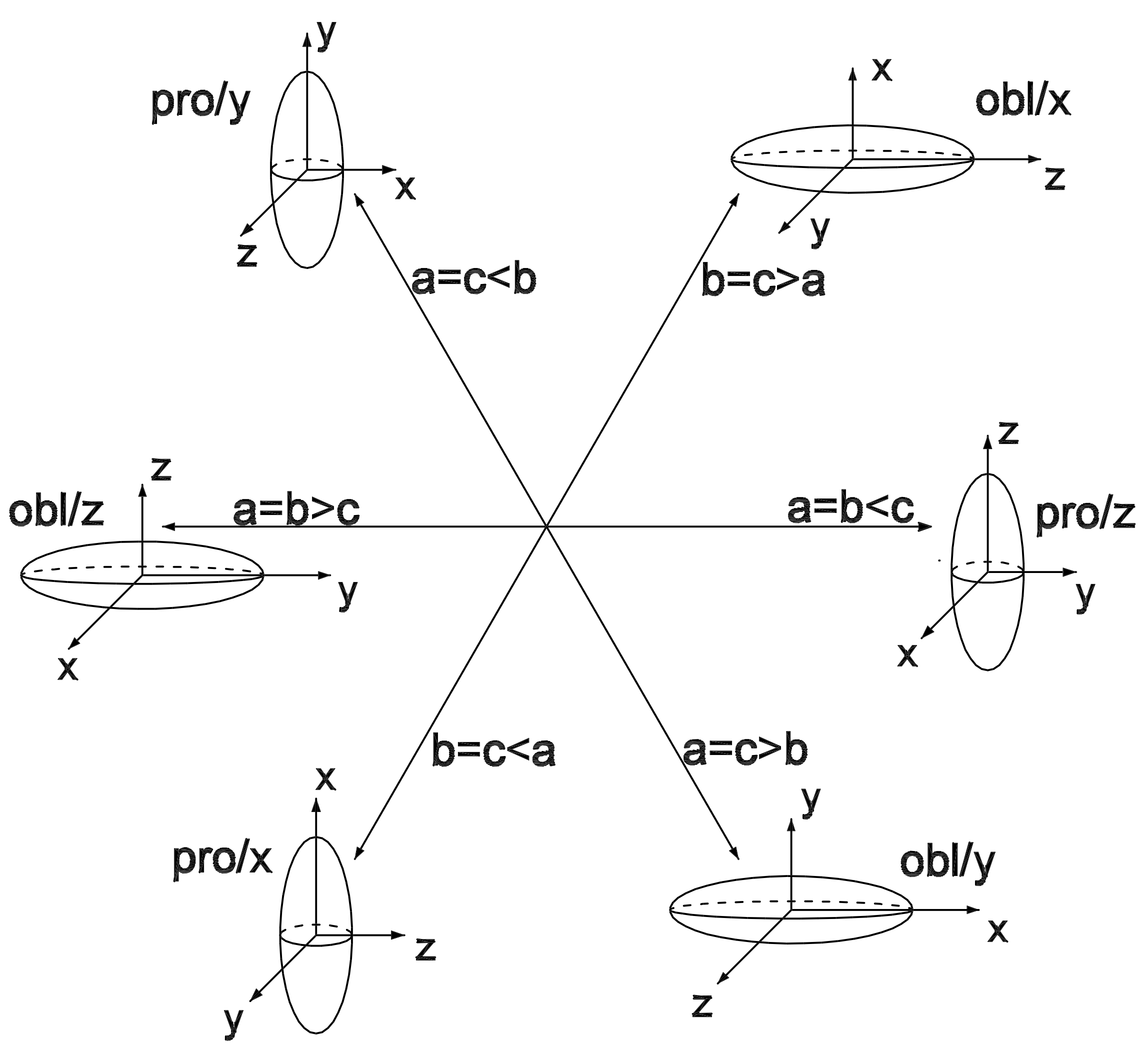

pro/y
obl/x
a=c<b
b=c>a
obl/z
a=b>c
a=b<c
pro/z
b=c<a
a=c>b
pro/x
obl/y

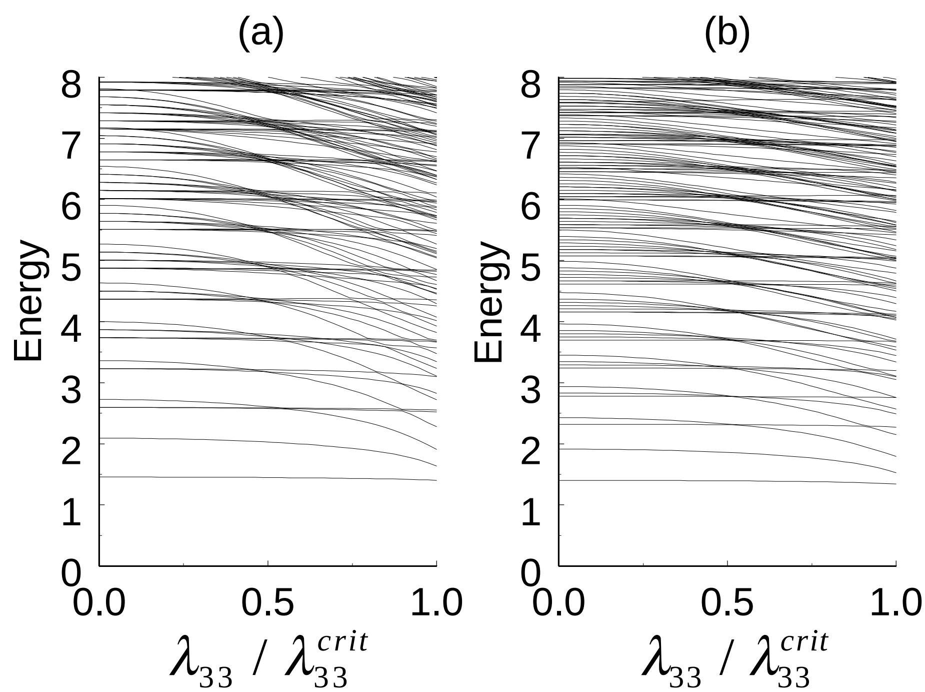

(a)
(b)
Energy
Energy
8
7
6
5
4
3
2
1
0
0.0
0.5
1.0
λ_{33} / λ_{33}^{crit}
λ_{33} / λ_{33}^{crit}

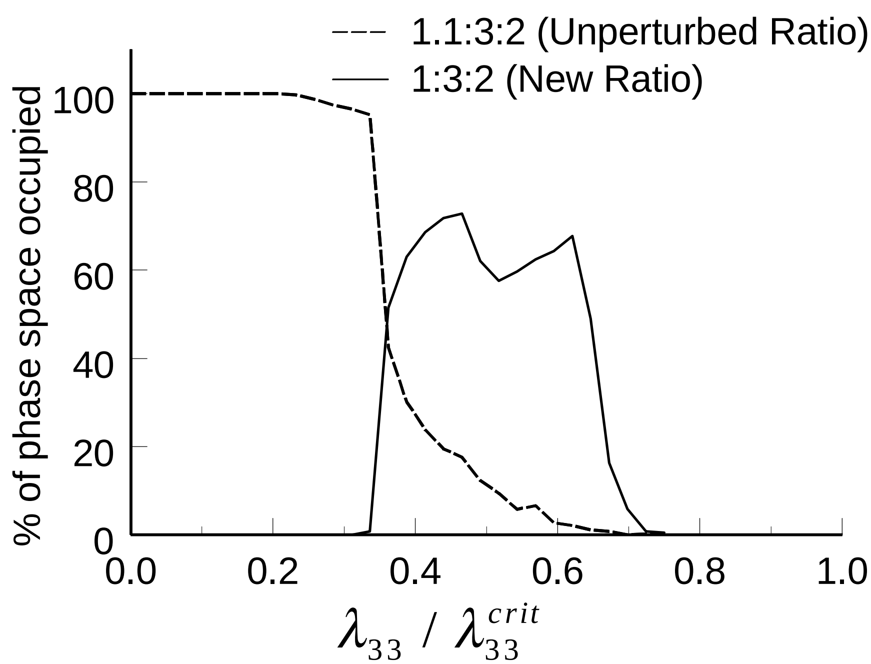
1.1:3:2 (Unperturbed Ratio)
1:3:2 (New Ratio)
% of phase space occupied
100
80
60
40
20
0
0.0
0.2
0.4
0.6
0.8
1.0
$\lambda_{33} / \lambda_{33}^{crit}$

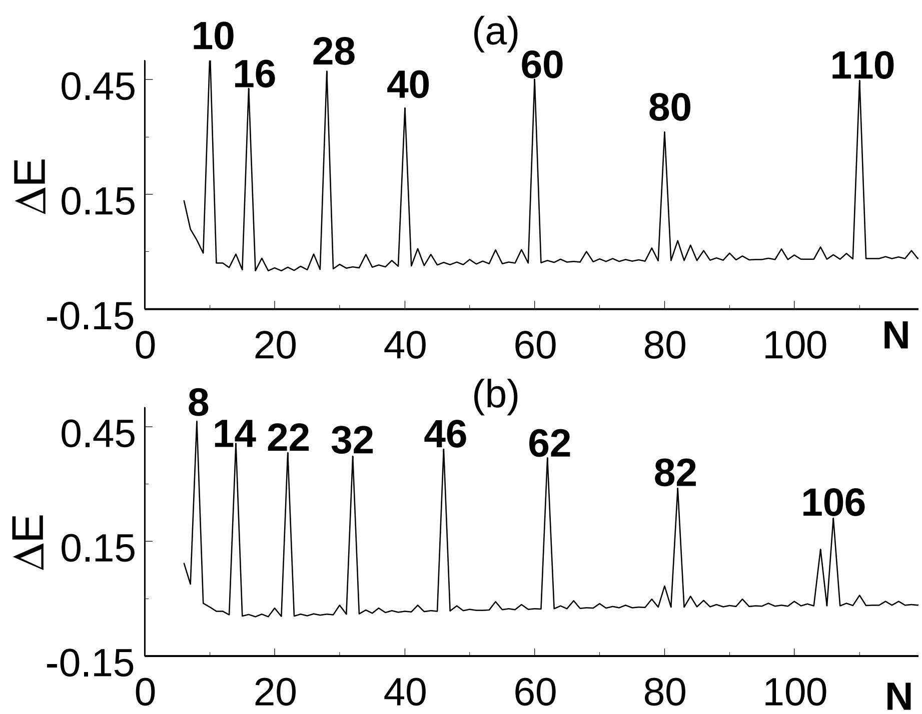

(a)
10
16
28
40
60
80
110
0.45
0.15
-0.15
ΔE
0
20
40
60
80
100
N
(b)
8
14
22
32
46
62
82
106
0.45
0.15
-0.15
ΔE
0
20
40
60
80
100
N